

## Effects of Different Swimming Exercise Intensities on Bone Tissue Composition in Mice: A Raman Spectroscopy Study

Fabiano Fernandes da Silva, M.Sc.,<sup>1</sup> Renato Aparecido de Souza, Ph.D.,<sup>1</sup>  
Marcos Tadeu Tavares Pacheco, Ph.D.,<sup>2</sup> Wellington Ribeiro, Ph.D.,<sup>3</sup>  
Marcos Augusto Souza Rodrigues da Silva, M.Sc.,<sup>2</sup> Humberto Miranda, Ph.D.,<sup>4</sup>  
Miguel Angel Castillo Salgado, Ph.D.,<sup>5</sup> Julio Cezar de Melo Castilho, D.D., Ph.D.,<sup>5</sup>  
and Landulfo Silveira, Jr., Ph.D.<sup>2</sup>

### Abstract

**Objective:** Raman spectroscopy was employed to evaluate the effect of different swimming intensities on femoral bone composition in an animal model. **Background Data:** Intense swimming exercise may affect bone mineralization, and Raman technique has been shown to be effective in evaluating tissue composition (phosphate minerals and carbonate apatites – bands at 960 and 1170  $\text{cm}^{-1}$ , as well as collagen matrix – amide I band at 1660  $\text{cm}^{-1}$ ). **Materials and Methods:** Eighteen female Swiss Webster mice were separated into three groups ( $n = 6$  per group) of sedentary (SED), and swimming with an intensity of 40% (PT-40) and 80% (PT-80) of the maximum load, with 6 weeks of training. Near-infrared Raman spectra (830 nm wavelength and 80 mW laser power) were obtained with a dispersive Raman spectrometer using a CCD camera and imaging spectrograph with 30-s integration time. Spectra were collected in the medial and lateral diaphysis of the femur and principal components analysis (PCA) was employed to extract features of the Raman bands of bone and to perform quantitative analysis. **Results:** PC1 vector resembles Raman spectra and carries information about apatite minerals and some contribution from organic matrix. A statistically significant difference was found in the PC1 scores (ANOVA,  $p < 0.05$ ), indicating lower mineral concentrations in the femur in both the PT-40 and PT-80 groups compared to the SED group. These results corroborated with the radiographic assessment of bone density. **Conclusion:** Raman technique associated with PCA statistics showed that intense swimming exercise may affect bone mineralization and remodeling in a mouse model of training.

### Introduction

BIOMEDICAL LITERATURE HAS REPORTED THAT the mechanical loading generated by physical activities plays an important role in bone development.<sup>1–4</sup> Due to the lack of bone mechanical loadings, reduced osteoid and mineralizing surfaces and decreased bone formation rate have been reported in space flight experiments,<sup>5</sup> and a similar effect of bone mass loss has been reported in scuba divers.<sup>6</sup> Physical training increases the cancellous bone and

osteoinductive activity due to an increase of bone morphogenic proteins (BMPs), which decreases bone resorption and increases bone formation.<sup>7</sup> Physical activity could be considered a strategy to reduce the risk of osteoporosis, leading to decreased bone fragility and reduced risk of fracture.<sup>8,9</sup>

Studies have shown that bone mineral density (BMD) is an indicator of bone health and could be used to assess the bone mineralization and mechanical properties in both experimental models<sup>10–12</sup> and humans.<sup>6,13</sup> Resistance training such

<sup>1</sup>Grupo de Estudo e Pesquisa em Ciência da Saúde (GEP-CS), Instituto Federal de Educação, Ciência e Tecnologia do Sul de Minas – Campus Muzambinho, Bairro Morro Preto, Muzambinho, MG, Brazil.

<sup>2</sup>Biomedical Engineering Center, Universidade Camilo Castelo Branco - UNICASTELO, Núcleo do Parque Tecnológico de São José dos Campos, São José dos Campos, SP, Brazil.

<sup>3</sup>Institute of Research and Development (IP&D), Universidade do Vale do Paraíba-UNIVAP, São José dos Campos, SP, Brazil.

<sup>4</sup>School of Physical Education and Sports, Universidade Federal do Rio de Janeiro—UFRJ, Rio de Janeiro, RJ, Brazil.

<sup>5</sup>Faculdade de Odontologia de São José dos Campos, Universidade Estadual Paulista – UNESP, São José dos Campos, SP, Brazil.



as running and swimming with weight bearing has been shown to improve BMD in the growing bone of rats,<sup>10</sup> and resistance muscle training may also improve the beneficial effects of BMD in post-menopausal women, particularly in association with hormone therapy.<sup>13</sup> Swimming may have a beneficial effect on BMD compared to the controls for elderly animals with induced osteoporosis.<sup>14</sup> On the other hand, weightlessness or skeletal unloading such as swimming may not have an equivalent beneficial effect on BMD when compared to weighted training,<sup>10</sup> or could lead to bone loss in rats with hypertension-induced osteoporosis<sup>12</sup> and healthy scuba-divers.<sup>6</sup> The prescription of water activities has been traditionally adopted as a preventive tool for bone health in the elderly,<sup>15,16</sup> but studies demonstrated that over-training and compulsive exercise could lead to pronounced loss of bone minerals.<sup>17,18</sup> Prolonged swimming training leads to a decrease in BMD, with stimulation of bone resorption in healthy rats<sup>11</sup> and in hypertensive rats with induced spontaneous osteoporosis.<sup>13</sup>

Different methods have been employed to evaluate bone density. Radiographic examination is an important clinical tool because it is non-invasive and can be easily performed. Taba et al.<sup>19</sup> showed a radiographic method based on grey-level analysis using image software to assess the bone density, with results similar to the histopathology. Bone composition can be assessed by Dual X-ray Absorptiometry (DXA), which provides a quantitative measurement of the mineral phase.<sup>20</sup> Bone is a composite material, and since the quality of the bone critically depends on both organic (primarily collagen I) and mineral phases,<sup>21</sup> and the organic phase remains essentially transparent to X-rays, there is a need for a technique that, in addition to measuring the bone mineral, could assess the collagen from bone matrix.

Raman spectroscopy is a vibrational technique that provides information on the chemical composition of organic and inorganic samples, allowing less invasive and nondestructive qualitative and quantitative analysis.<sup>22,23</sup> It has been considered effective in assessing sample information at the molecular level, and has been used for several minimally and non-invasive applications of biological samples such as detecting glucose in urine,<sup>24</sup> atherosclerosis in coronary and carotid arteries,<sup>25,26</sup> hepatitis C in human blood serum in vitro,<sup>27</sup> lactate identification in blood,<sup>28</sup> osteoinduction in biomaterial implants,<sup>29</sup> several bone diseases,<sup>30</sup> and bone synthesis and osteointegration after healing,<sup>31,32</sup> as well as evaluating the microstructure of human cortical bone (osteon).<sup>33</sup> Several works have proposed the use of Raman spectroscopy to determine the mineralization and organic matrix to assess bone quality.<sup>30,34–36</sup> Raman spectroscopy has been demonstrated by many authors as a tool for the study of bone mineralization<sup>34,35</sup> and has emerged as an important complement to traditional methods for detection, quantification, and imaging of local variations in the molecular structures of bone matrix and minerals.<sup>30</sup> Also, it has been demonstrated that the Raman spectrum could be obtained transcutaneously, accurately assessing bone tissue composition through the skin in live mice.<sup>37</sup>

At least two different aspects of the mineral components of bone affect its mechanical properties: degree of remodeling and bone mineral density (mineral-to-matrix phase ratio) and degree of crystallinity of the mineral content.<sup>30</sup> The crystallinity, which is related to the mineral quality and is an

important quality factor for bone tissue, has been correlated to the carbonate/phosphate ratio and indicates the extent of carbonate incorporation in the hydroxyapatite lattice.<sup>35</sup> Those parameters of bone tissue could be assessed by the ratios between selected Raman bands of interest. Femoral trabecular bone showed a higher mineral-matrix ratio in women who had sustained a fracture rather than in women without a fracture, while iliac crest biopsies revealed a higher carbonate-phosphate ratio in cortical bone of women who had sustained a fracture.<sup>38</sup> Also, bones from postmenopausal osteoporotic patients were found to have a lower mineral-matrix ratio and higher carbonate-phosphate ratio when compared to normal patients.<sup>39</sup>

The aim of this study was to assess the composition of bone tissue (mineral and organic phases) in vitro at the medial and lateral diaphysis of the femur in swimming-trained healthy young mice compared to sedentary animals over 6 weeks of training, in order to evaluate the effects of different swimming-training intensities on bone metabolism (BMD) of mice. Dispersive Raman spectroscopy at 830 nm was performed in order to evaluate the mineral phase (phosphate and carbonate apatite bands at 903–991 cm<sup>-1</sup> and 1046–1110 cm<sup>-1</sup> Raman shifts respectively) and the organic phase (collagen matrix: amide I band at 1620–1680 cm<sup>-1</sup> Raman shift). Also, principal components analysis (PCA) was employed to extract quantitative information from Raman spectra by correlating of the radiographic assessment of bone density and the ratio of carbonate/phosphate bands with the scores of PCA.

## Materials and Methods

### Experimental model

Eighteen young adult Swiss Webster female mice (3 months old, 35.0 ± 0.3 g) were obtained from the bioterium of the Institute of Biomedical Sciences – Universidade de São Paulo (São Paulo, SP, Brazil). Mice were kept in plastic cages (49 cm length × 34 cm width × 16 cm height; 10 animals per cage) in a room with controlled environmental conditions (22–25°C, relative humidity 40–60%, 12-h light–dark cycle) prior to swimming training. Moreover, all animals had access to palletized food (Labina Chow, Purina, SP, Brazil) and water ad libitum. Animals were equally separated into three experimental groups (*n* = 6 per group): sedentary (SED), non-exercised animals; trained animals submitted to the swimming protocol with an intensity equal to 40% of the maximum load (PT-40); trained animals submitted to the swimming protocol with an intensity equal to 80% of the maximum load (PT-80), in a swimming protocol for 6 weeks. Experimental procedures were done according to the principles for animal handling and care recommended by the COBEA (Brazilian School of Animal Experimentation) and approved by the Committee on Ethics in Research (UNIVAP – Protocol # A106/CEP/2007).

### Swimming-training protocol

Animals in the trained group were submitted to a period of swimming adaptation (30 min daily without load, during five consecutive days) in a 250-L water-filled bath with the temperature kept at 35 ± 2°C in order to decrease the stress of the swimming activity.<sup>9,40</sup> After adaptation, the animals



were individually submitted to a test of maximum load,<sup>41,42</sup> which consisted of lead load cells corresponding to 1%, 2%, 3%, and so forth, of the total body weight of the animal, attached to the animal's chest with the help of a comfortable vest. The animal was left in the bath to swim until it was exhausted, reaching the maximum tolerated load with such lead loads.<sup>40–42</sup> The animal's exhaustion was determined by its inability to stay above the surface of the water for approximately 8 s.<sup>41,42</sup> This test allowed the adjustment of the working load for the physical training to 40% (PT-40) and 80% (PT-80) of the maximum load. The swimming-training sessions were performed in groups of six animals because exercise becomes more vigorous in animals grouped together than in individual swimming.<sup>40</sup> These 30-min training sessions occurred every workday.<sup>10</sup> At the end of each experimental week, body weight was taken and new maximum load test was performed for possible training load readjustments.

### Bone samples

All animals were anesthetized with intramuscular administration of 40 mg/kg of xylazine HCl (Xilazin 2%, 50 mL; Syntec do Brasil Ltda., São Paulo, Brazil) and 50 mg/kg of ketamine HCl (Cetamin 10%, 50 mL; Syntec do Brasil Ltda.) and euthanized with an intracardiac injection of KCl solution (Cloreto de potássio 10%; Laboratório Ariston Ltda., São Paulo, Brazil). The animals were aged 15 weeks at this time. The right femur was harvested and all visible soft tissues were removed; the femurs were then wrapped in aluminum foil and frozen in liquid nitrogen ( $-196^{\circ}\text{C}$ ), since chemical fixation is not advisable for Raman studies.<sup>26,32</sup> Before Raman spectroscopy and digital optical density measurements, bone samples were warmed to room temperature with 0.9% saline.

### Dispersive Raman system

For Raman measurements, a near-infrared dispersive Raman spectrometer was used, as shown in Fig. 1a and described elsewhere.<sup>28,32</sup> Briefly, a semiconductor laser (L4830S; Micro Laser Systems, Inc., Garden Grove, CA) with an output power of  $\sim 80$  mW and a wavelength of 830 nm was used to excite the bone fragments held by a metal sampler. The laser beam was directed to the sample holder by a quartz prism before being focused by an  $f = 25$  mm lens. The signal scattered from the samples was collected by a set of lenses and was coupled to the entrance of the spectrograph (250IS, 600 lines/mm grating; Chromex, Inc., Wal-

tham, MA) for dispersion, which had a notch filter at 830 nm (PN-ZX 000080; Iridian Spectral Technologies, Inc., Ontario, Canada) in front of the entrance slit. The spectrograph had a spectral resolution of about  $10\text{ cm}^{-1}$ . The signal dispersed by the spectrograph was detected by a CCD (charge-coupled device) camera and controller (LN/CCD-1024-EHR1 –  $1024 \times 256$  pixels, and ST-130; Princeton Instruments, Inc., Trenton, NJ) connected to a computer. Each sample was scanned on the same day and in the same experimental conditions. The Raman signal was collected in 30 s for all 18 bone samples. Two spectra were acquired on the surface of the middle third of medial and lateral diaphysis of each femur (as seen in Fig. 1b).

Raman shift calibration and spectra pre-processing were done following the procedures described elsewhere.<sup>32</sup> Basically, bands from naphthalene were measured and a third-order polynomial function was calculated by correlating the pixel position with the band position ( $\text{cm}^{-1}$ ). The fluorescence background and CCD readout noise were removed from the original spectrum by fitting and subtracting a fifth-order polynomial to the raw data in the spectral region of  $800\text{--}1800\text{ cm}^{-1}$ , allowing the visualization of the peaks found in the bone.

### Digital optical density

In order to correlate the Raman measurements, the bone optical density was measured by means of a CCD (Visualix GX-S-HDI™, Gendex Dental Systems, Des Plaines, IL) for collecting digital X-ray radiographs.<sup>43</sup> First, CCD and bone samples were stabilized in a standard fixing device. Afterwards, each femur was radiographed with X-ray equipment (Spectro-70X™; Dabi Atlante, São Paulo, Brazil) at 10 mA and 65 kVp, with 0.1 s exposure time and 40 cm focus-object distance. Radiographs were taken from both sedentary and exercised groups, and digital images were acquired and transferred to the computer. The bone optical density was evaluated using the VixWin™ 1.4 system (Gendex Dental Systems, Inc.). Image resolution was 635 pixels per inch (ppi), image size was  $900 \times 641$  dpi, and pixel size was 40  $\mu\text{m}$ . Images were stored in TIFF format without compression with a resolution of 600 dpi. The images were imported to image software (Adobe Photoshop 6.0; Adobe Systems, Inc., San Jose, CA) on a PC and displayed on a monitor with  $1024 \times 768$  pixel resolution. BMD was evaluated using a grey-level histogram in an area of  $5 \times 5$  pixels for all bones. All the results were expressed in 8-bit grey levels (0–255).<sup>44</sup>

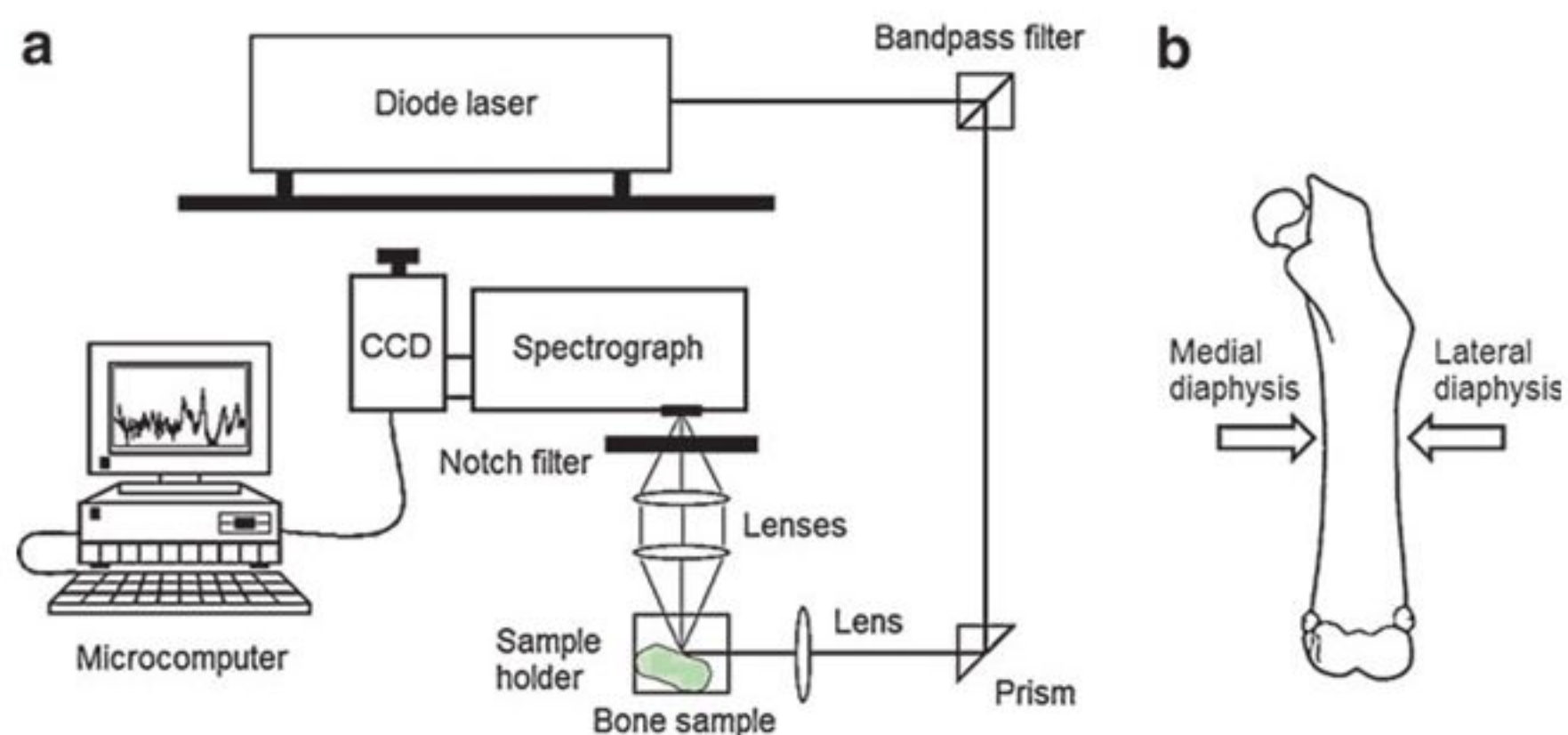


**FIG. 1.** (a) Schematic diagram of the dispersive, near-infrared Raman spectrometer. Laser power: 80 mW; wavelength: 830 nm; resolution:  $10\text{ cm}^{-1}$  with  $150\text{ }\mu\text{m}$  slit width. (b) Indication of the place on the bone where the Raman measurement was taken.



### Statistical analysis

Statistical analysis was performed using two approaches. First, PCA<sup>45</sup> was applied to the Raman spectra in order to obtain a quantitative analysis of the general amount of mineral and organic matrix of the analyzed samples depending on the training, by using the scores of the first and second principal components, which represent the information of organic and inorganic phase. Second, intensity and ratio analyses of selected bands were performed, in which the mean value of the intensities of three characteristic bands were measured: phosphate and carbonate apatites (903–991  $\text{cm}^{-1}$  and 1046–1110  $\text{cm}^{-1}$ , respectively), representing the mineral content, and collagen matrix (amide I, 1620–1680  $\text{cm}^{-1}$ ) representing the organic content. Ratios of these band intensities resulted in relative measurements of carbonate–phosphate, phosphate–protein, and carbonate–protein ratios.<sup>38</sup> Data were expressed as mean  $\pm$  standard deviation. PCA calculation was done using the program ProRaman<sup>46</sup> under Matlab 4.01 software (The Mathworks, Inc., Natick, MA).

One-way ANOVA was used to evaluate the body weight changes, the differences in the PCA scores, the Raman band ratios, and the bone optical density, depending on the training intensity among the three experimental groups. A post-hoc analysis (Tukey–Kramer test) was used to determine the location of significant differences when necessary. Differences among groups were considered statistically significant when  $p < 0.05$ . To correlate the Raman findings with the bone optical density, the Pearson correlation coefficient was calculated for density and bands/PCA scatter plots using the data from each experimental group. ANOVA was done using InStat (30-day trial version; Graphpad Software, Inc., La Jolla, CA).

## Results

### Body weight

Figure 2 shows the body weight (mean and standard deviation) for all groups at the beginning and end of training. All experimental groups had similar initial body weights. At the end of the 6-week training period, the increase in body weight of both exercise groups was less than in the control group, with the mice in PT-40 and PT-80 groups exhibiting mean body weights that were about 9.6% and 10.9% less

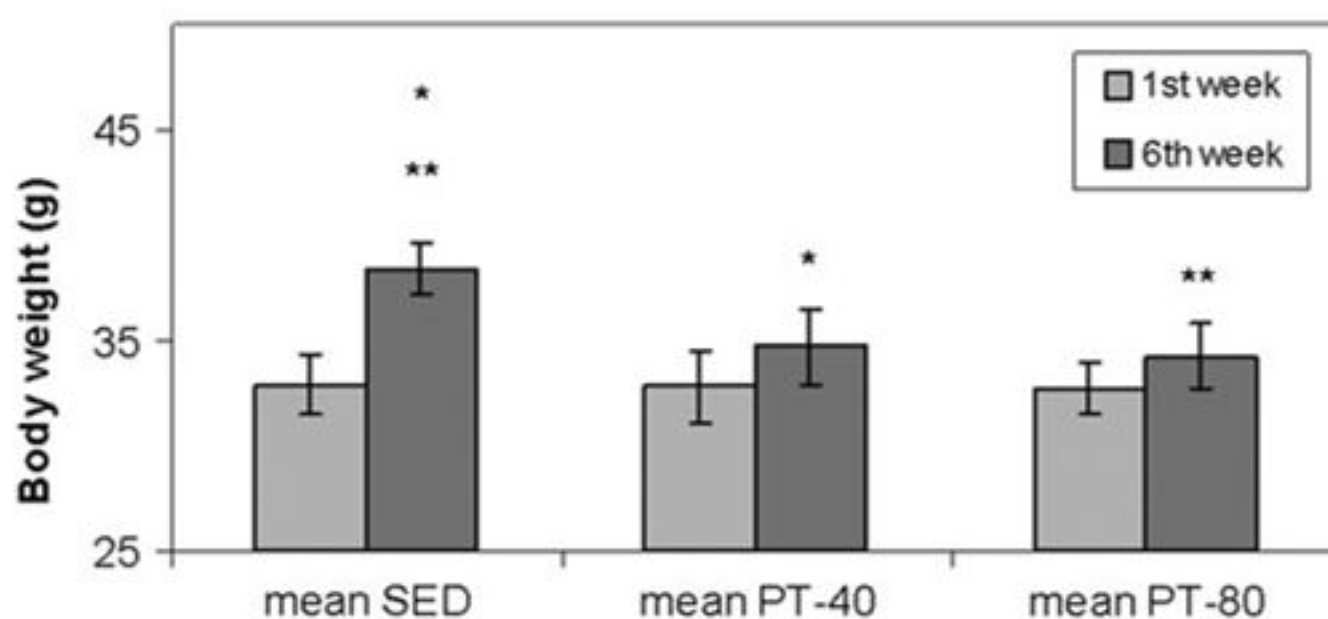


**FIG. 2.** Comparison of the initial and final mean and standard deviation of body weight during the experimental period. \* and \*\* indicate SED group with a significantly higher body weight than the physical training groups at the end of study ( $p < 0.05$ ).

than those of the SED mice respectively ( $p < 0.05$ ). There were no statistically significant differences in mean body weight between the two exercise groups at any time points during the training period.

### Raman spectral analysis

Raman spectra of the bone showed prominent vibrational bands of organic and inorganic compounds related to bone tissue composition. Figure 3 shows the mean Raman spectra of each diaphysis femoral points obtained for the SED, PT-40, and PT-80 groups. The main bands are found at  $\sim 960 \text{ cm}^{-1}$ , attributed to phosphate apatite ( $\text{PO}_4$  stretching);  $\sim 1070 \text{ cm}^{-1}$ , attributed to carbonate apatite ( $\text{CO}_3$  stretching); and  $\sim 1660 \text{ cm}^{-1}$ , attributed to amide I stretching from the matrix collagen.<sup>30–32</sup> Figure 3 illustrates differences in the intensity of the selected Raman bands in all experimental groups, mainly in the SED group, which had higher intensity compared to PT-40 and PT-80.

In order to evaluate the differences in the Raman spectra of bone tissues related to the amount of mineral and organic phases, two analyses were performed. First, PCA was applied to all Raman spectra of diaphysis femoral points, and the first two principal components scores were then used to correlate those differences to the training status of the animals, depending on the spectral information found in the principal component vectors. Second, ratios between organic

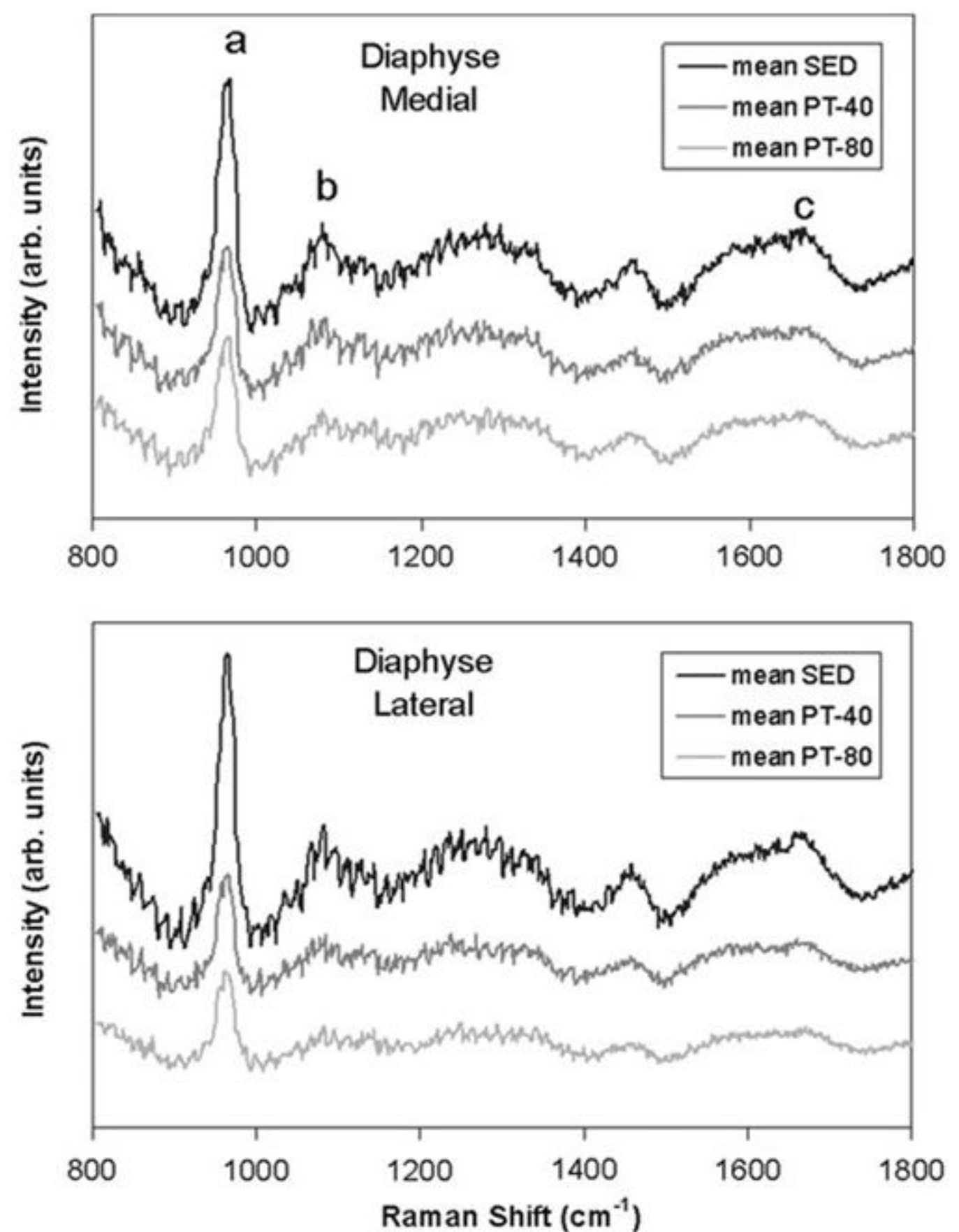


**FIG. 3.** Raman spectra of diaphysis bone. Main bands are indicated: (a) phosphate apatite ( $960 \text{ cm}^{-1}$ ); (b) carbonate apatite ( $1070 \text{ cm}^{-1}$ ); (c) amide I from the collagen matrix ( $1660 \text{ cm}^{-1}$ ).



and inorganic phases (carbonate, phosphate, and protein bands) were calculated to detect the degree of remodeling and bone quality.

In the PCA analysis, the score values and the respective loading vectors for the first two principal components of the experimental group were obtained using all spectra. Figure 4 presents the PC1 and PC2 spectral vectors. PC1 shows most of the spectral information originating from apatite minerals (calcium hydroxyapatite:  $960$  and  $1070\text{ cm}^{-1}$  bands) and some contribution from organic matrix (collagen-proteins:  $1660\text{ cm}^{-1}$  band). PC2 presents the spectral information from the  $960\text{ cm}^{-1}$  band and some remnants from the background fluorescence at  $1500\text{--}1700\text{ cm}^{-1}$ .

ANOVA statistical analysis of the PC1 scores of both sites (mean of diaphysis medial and lateral sites) evidenced that the concentrations of calcium hydroxyapatite in both PT-40 and PT-80 groups were significantly lower than the SED group ( $-45\%$  and  $-50\%$  respectively,  $p < 0.05$ ; Fig. 5). For PC2, no statistically significant difference was found among groups.

For remodeling evaluation, the ratio between carbonate-phosphate ( $1070/960\text{ cm}^{-1}$ ), phosphate-protein ( $960/1660\text{ cm}^{-1}$ ), and carbonate-protein ( $1070/1660\text{ cm}^{-1}$ ) were calculated using the Raman band intensities.<sup>40</sup> Figure 6 presents the ratios for the diaphysis medial and lateral sites. Although the ratios differences were not statistically significant, the study found: (1) a higher carbonate-phosphate ratio in the PT-40 and PT-80 groups than in the SED mice (Fig. 6a); (2) a lower phosphate-amide I ratio in the PT-80 and PT-40 groups than in the SED mice (Fig. 6b); and (3) lower carbonate-protein in the PT-80 and PT-40 groups than in the SED mice (Fig. 6c). A high carbonate-phosphate ratio was generally associated with a low phosphate-protein and carbonate-protein ratio, and vice versa (Fig. 6).

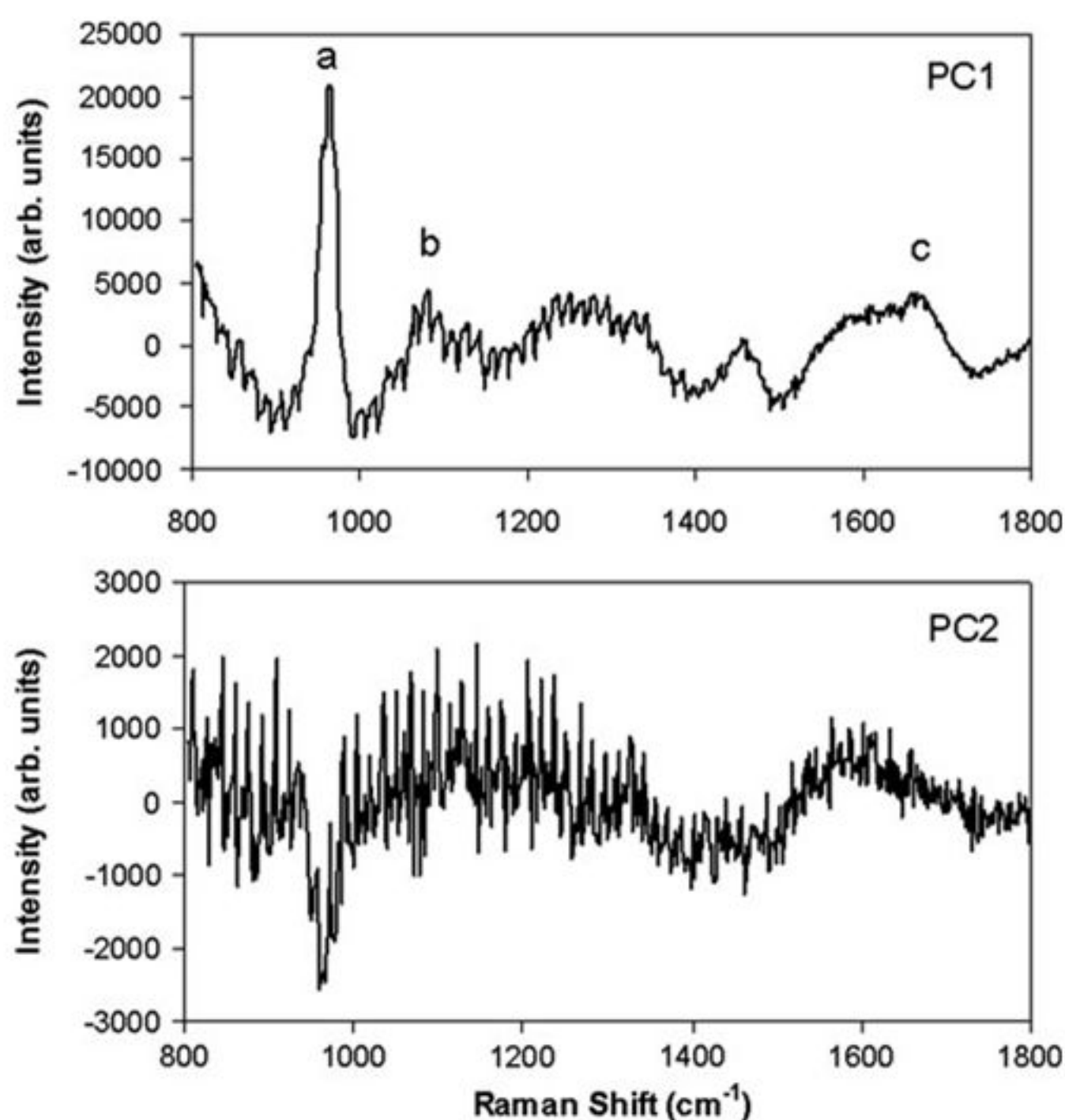


FIG. 4. Principal components PC1 and PC2 loading vectors for the diaphysis medial and lateral sites. Features a–c as labeled in Fig. 3.

#### Digital optical density

The bone optical density in the cortical region showed no statistically significant differences between the experimental groups. Although not significant, the sedentary group presented a higher value in relation to the PT-40 group, and the PT-40 showed a higher value in relation to the PT-80 group (Fig. 7).

Figure 8 plots the mean PC1 score and the mean intensity ratio of phosphate-protein with the corresponding mean bone optical density (Fig. 8a). Also, the scatter plot of the carbonate was plotted with the corresponding PC2 score (Fig. 8b). Despite the high standard deviations, the plots showed a high correlation.

#### Discussion

This work proposed the study of bone composition in swimming-trained mice using dispersive Raman spectroscopy. The objective was to compare the relative amount of mineral content and the collagen matrix to the assessment of bone optical density and bone quality after 6 weeks of swimming training compared to sedentary mice. The Raman technique was selected because Raman has been used to access the molecular structure of bone mineral and organic components nondestructively.<sup>30</sup>

Many methods used to study bone are unable to give information at the molecular level.<sup>21,25</sup> Raman spectroscopy has the advantage of being sensitive to both the mineral and organic components of bone, thus allowing the study of mineral-matrix interactions, as well as the individual properties of each component.<sup>30,34–36</sup> Phosphate P–O symmetric stretch attributed to phosphate apatite ( $960\text{ cm}^{-1}$ ), carbonate C–O symmetric stretch attributed to carbonate apatite

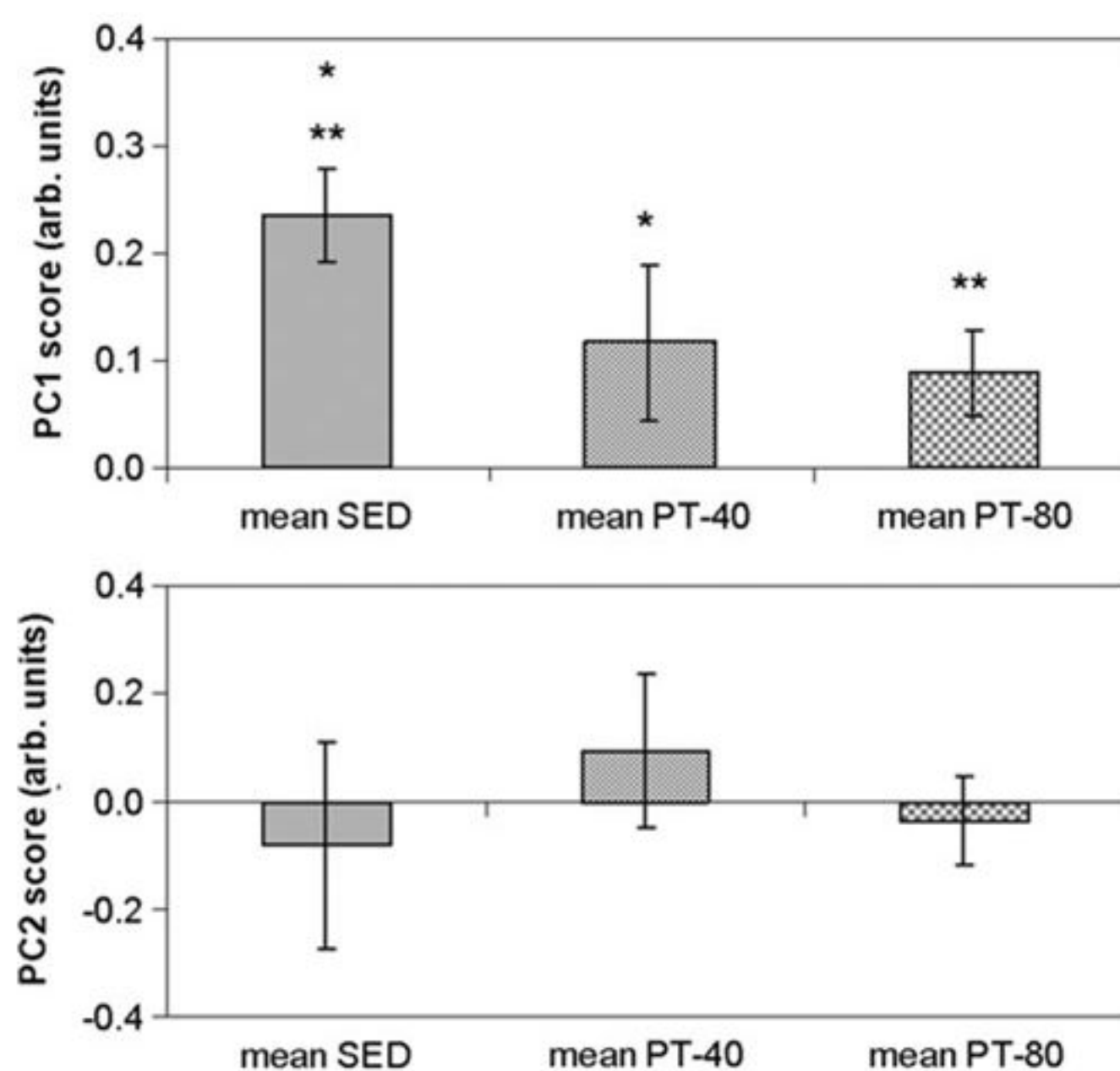


FIG. 5. Mean intensity and standard deviation for the principal components scores PC1 and PC2 of the diaphysis medial and lateral sites. \* and \*\* indicate SED group with a statistically significant difference than the physical training groups PT-40 and PT-80 respectively ( $p < 0.05$ ).



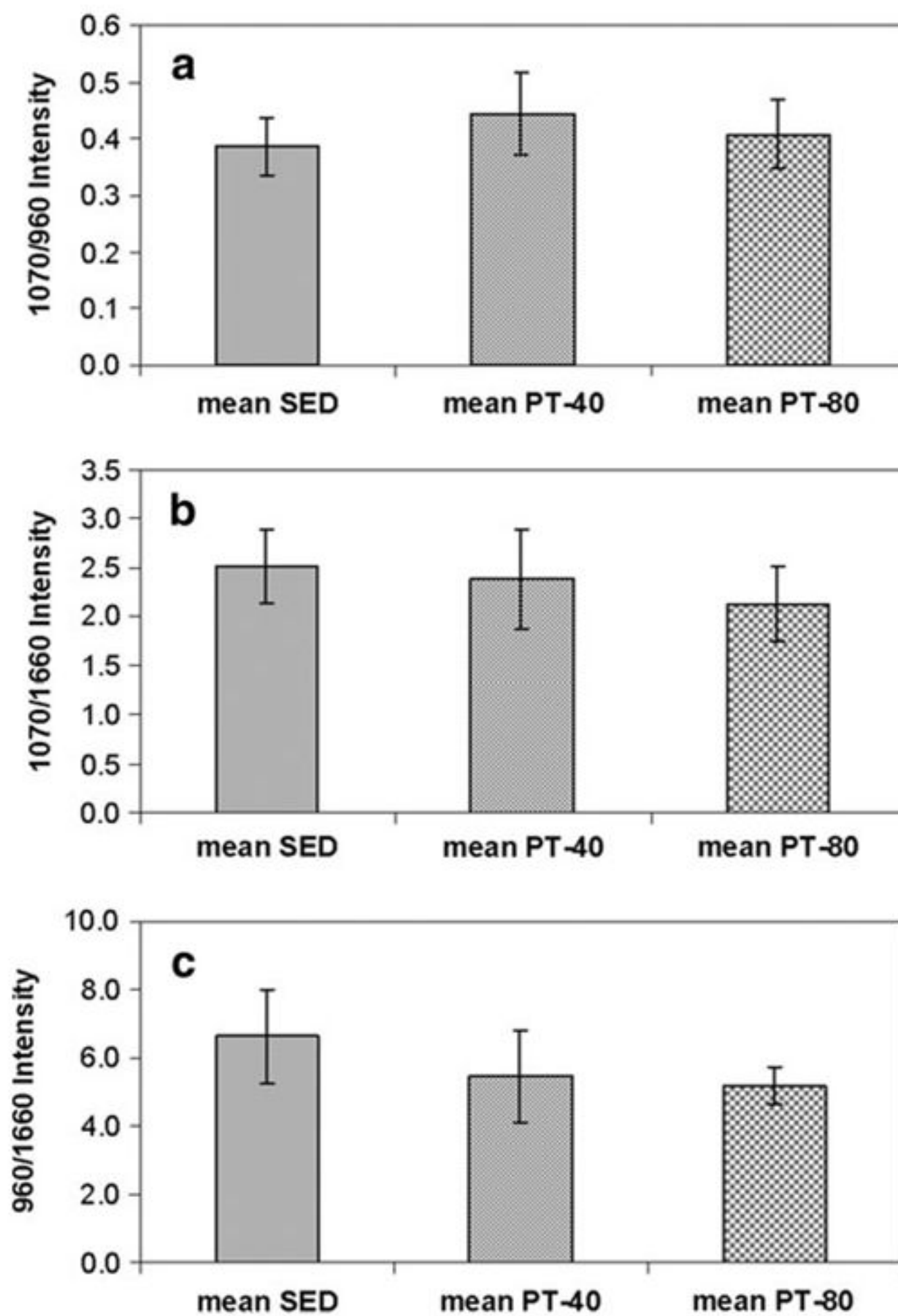


FIG. 6. Intensity ratio between (a) carbonate-phosphate ( $1070/960\text{ cm}^{-1}$ ), (b) phosphate-protein ( $960/1660\text{ cm}^{-1}$ ), and (c) carbonate-protein ( $1070/1660\text{ cm}^{-1}$ ) for the diaphysis medial and lateral sites. Differences between groups were not statistically significant.

( $1070\text{ cm}^{-1}$ ), and collagen amide I from the organic matrix ( $1660\text{ cm}^{-1}$ ) were used as markers of phosphate, carbonate, and organic matrix respectively.<sup>30</sup> It was possible to demonstrate that the Raman spectrum of the bone shows clearly the prominent vibrational bands related to biomarkers (Fig. 3).

In this study, the evaluation of bone mineralization and organic phase was done quantitatively through PCA and

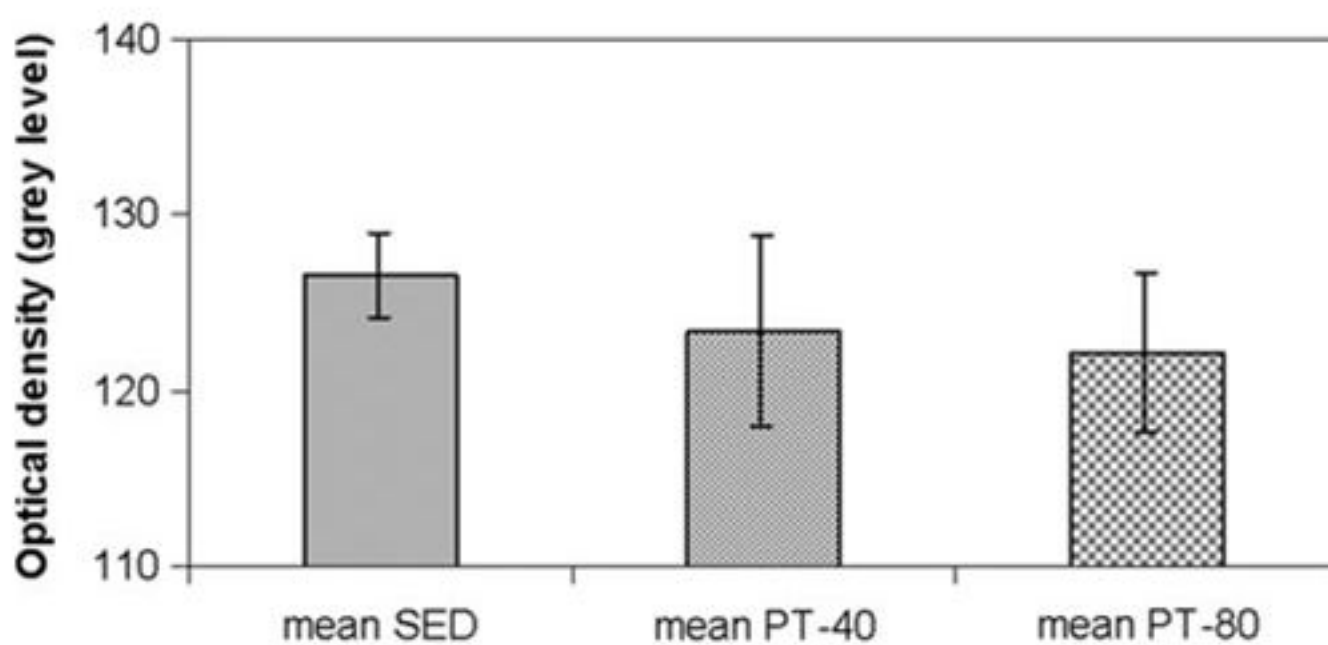


FIG. 7. Mean of radiographic cortical optical density of SED and trained groups. Differences between groups were not statistically significant.

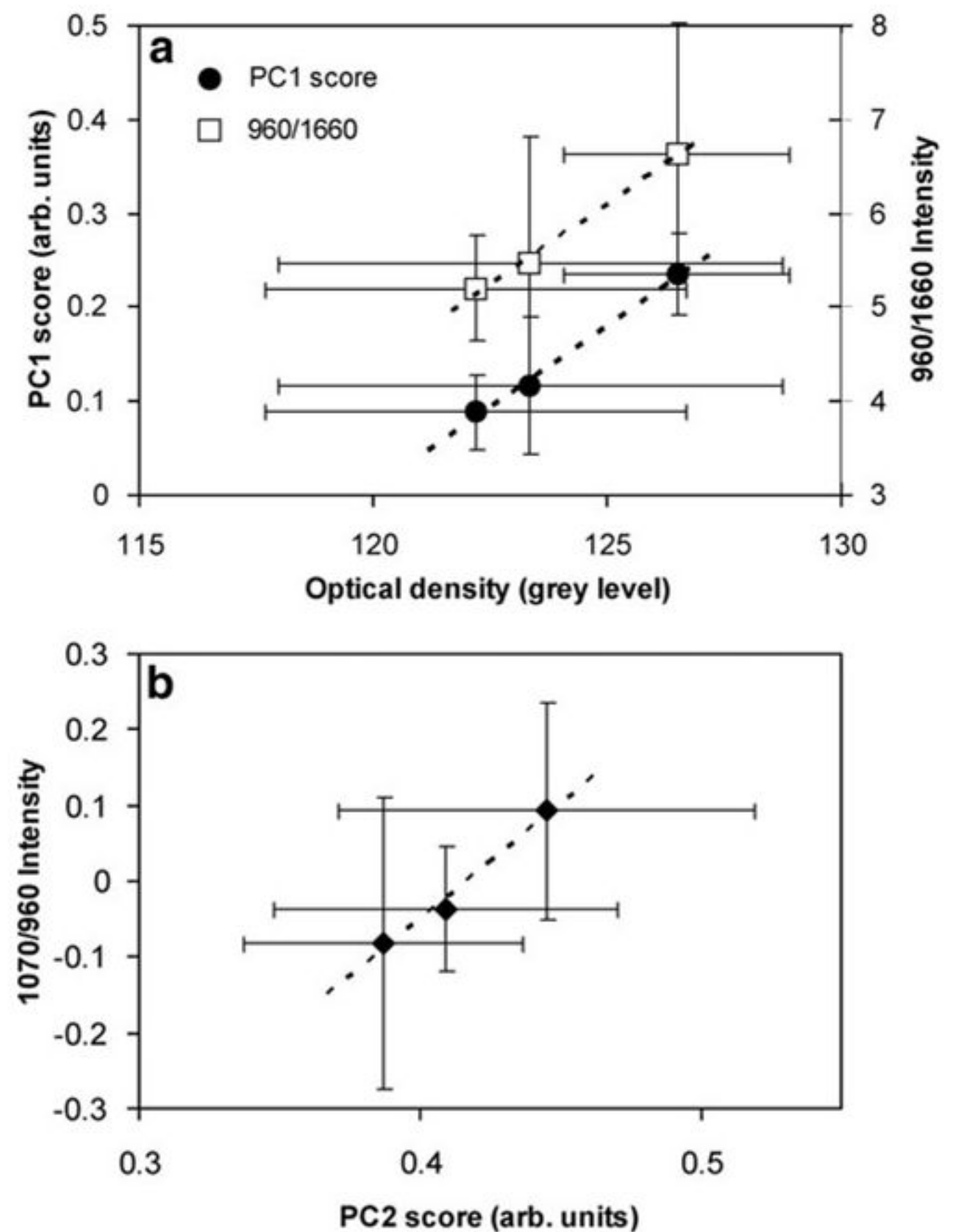


FIG. 8. (a) Scatter plot between PC1 score and phosphate-protein ratio with the corresponding bone optical density; (b) scatter plot between carbonate-phosphate ratio with the corresponding PC2 score.

band intensity ratio analysis respectively, applied to all Raman spectra of femoral bones. The PCA scores showed a statistically significant reduction in the concentrations of calcium hydroxyapatite in the swimming groups (PT-40 and PT-80) at the same anatomical location (diaphysis femoral points) compared to sedentary (Fig. 5), which was void to direct muscle attachments. Such difference suggests that a negative mechanical influence occurs after a regimen of intense non-weight bearing exercise at skeletal sites where the muscles are inserted.<sup>47</sup> These deleterious effects on bone promoted by the swimming training have been described in the literature.<sup>6,10,13,18</sup> Bourrin et al.<sup>18</sup> used an intense regimen that involved rats swimming for 6 h/day, which more closely resembles the regimen of collegiate swimmers at the peak of their training season. They found decrements in mineral bone status, which could be due to prolonged weightlessness in the water and/or prolonged exposure to stress hormones such as corticosterone. Using an animal model, Kim and Park<sup>11</sup> and Kim et al.<sup>13</sup> observed that prolonged swimming resulted in a decrease of BMD and bone strength compared to sedentary animals. The distinguishing characteristics of these exercises are strenuous intensity exercise.

It is important to note that, despite not being statistically significant, the results of the measurements of the bone digital optical density are encouraging (Fig. 7), as the same findings, the decrement in bone density concentration in



exercised groups, were shown by PCA analysis. Iwamoto et al.<sup>48</sup> reported that, although BMD of exercised rats showed no significant difference at 4 or 8 weeks from the beginning of exercise training, it began to show at 12 weeks. This finding might be the reason for no significant change of BMD in our swimming exercise group, where the experimental period was too short to alter this variable. It is also important to consider that PCA loading vectors present spectral information from apatite minerals (960 and 1070  $\text{cm}^{-1}$  bands) and some contribution from organic matrix (1660  $\text{cm}^{-1}$  band), while X-ray techniques rely on absorption only from the mineral phase. This aspect may have, in some way, affected the correlation between the Raman and the digital optical density findings (Fig. 8).

The ratio of phosphate-protein and carbonate-protein are directly proportional to the level of remodeling.<sup>30</sup> In the present study, the exercised groups had lower values for these ratios when compared to sedentary animals (Fig. 5b and c). With increased remodeling, a great amount of the existing bone tissue is relatively young. Because bone tissue continues to mineralize over time, this younger bone tissue contains relatively less mineral than older existing bone tissue. Thus the average mineral-matrix ratio tends to decrease when remodeling is increased.<sup>38</sup> In this context, higher remodeling in the exercised groups was observed. The tendency for the decrease in the mineral-matrix ratio during mechanical loading generated by physical activity is consistent with the hypothesis that increased remodeling occurs after training.<sup>7</sup> The increased remodeling may lead to bone tissue that is less resistant to fracture because it is not fully mineralized.<sup>38</sup> Thus the decreased mineral-matrix ratio found suggests that the lower bone density in exercised animal was a result of chemical changes in the bone tissue, perhaps as a result of increased remodeling without sufficient time for adequate mineralization.<sup>47,49</sup>

The difference in the carbonate-phosphate ratio may indicate a difference in the size of mineral crystals in the bone tissue, reflecting the crystallinity of the mineral content.<sup>34-36</sup> Although not statistically significant, the exercised animals had a higher carbonate-phosphate ratio when compared to sedentary animals (Fig. 6a). The carbonate-phosphate ratio appears to be a key variable in osteoporotic fracture. For instance, McCreadie et al.<sup>38</sup> and Boskey<sup>50</sup> observed a greater carbonate-phosphate ratio in iliac crest cortical bone from women with a fracture and with post-menopausal osteoporosis respectively. Thus the results represent differences that may be attributed to the quality of bone tissue and may add additional information about bone fragility and fracture risk (e.g., stress fracture related to the strenuous training).

Researchers agree that the physical activity presents beneficial effects on the bone, but results are still contradictory.<sup>6,10-14</sup> No significant difference in the maximum breaking force of the lumbar vertebral body was described among the exercise and control groups in mature osteopenic rats submitted to the strong physical activity, and that the beneficial effects of running exercise on weight-bearing bones with estrogen deficiency and inadequate calcium intake are reached only when an optimal level of exercise is applied.<sup>47</sup> Previous studies showed that different endurance training intensity levels led to differences in body weight and bone parameters of rats.<sup>11</sup> Depending on the type and intensity of exercise, as well as the animal's conditions, the effect on the

bone could be deleterious.<sup>47</sup> In terms of body weight, the results demonstrated that the exercise-training regimen reduced the gain of body weight in the exercised animals compared with the non-exercised controls (Fig. 2), similar to that reported in the literature.<sup>10,11,50</sup> These differences could be directly related to the training intensity,<sup>10,11,13</sup> low mechanical efficiency of the animal's swimming,<sup>47</sup> and the stress-related factors promoted by the swimming activity.<sup>41</sup> Therefore, the stress promoted by long duration and intense exercise results in elevated glucocorticoids for metabolic purposes (e.g., mobilization of free fatty acids, reducing the weight body).

Raman could be used to assess bone tissue composition and to evaluate the effects of different exercises and mechanical loading generated by physical activity in bone development and metabolism. New advances on fiber optic "Raman probes" and high resolution spectrometers may provide the valuable capability of detecting more subtle spectral differences even in vivo, transcutaneously,<sup>37</sup> and immediately after training, in a non- or minimally invasive way.

## Conclusion and Summary

Dispersive Raman spectroscopy may be a feasible method to quantify mineralization and remodeling in diaphysis femoral bone of mice submitted to an intense swimming protocol, by measuring the intensity of the mineral phase and ratio of the mineral and matrix phase. A decrease in the phosphate band, an increase in the carbonate-phosphate ratio, and a reduction in the phosphate-amide I, as well as the carbonate-protein ratios, in trained groups was found. Also, the scores of the PCA multivariate statistics showed a correlation with the BMD and carbonate-phosphate ratio values. Although not statistically significant, results indicated that the mineral phase is decreased and remodeling occurs at a higher rate in trained groups depending on the training intensity. The evaluation of bone mineralization by Raman/PCA analysis demonstrated that intense swimming exercise may be deleterious to bone status in healthy young mice.

## Acknowledgments

L. Silveira Jr. thanks CNPq (National Counsel of Technological and Scientific Development) for the Productivity Fellowship (305610/2008-2). The authors thank Fabiana Silva Pires for helping to train the experimental group.

## Author Disclosure Statement

No competing financial interests exist.

## References

1. Saxon, L.K., and Lanyon, L.E. (2008). Assessment of the in vivo adaptive response to mechanical loading. *Methods Mol. Biol.* 455, 307-322.
2. Plochocki, J.H., Rivera, J.P., Zhang, C., and Ebba, S.A. (2008). Bone modeling response to voluntary exercise in the hindlimb of mice. *J. Morphol.* 269, 313-318.
3. Greene, D.A., and Naughton, G.A. (2006). Adaptive skeletal responses to mechanical loading during adolescence. *Sports Med.* 36, 723-732.



4. Robling, A.G., Castillo, A.B., and Turner, C.H. (2006). Biomechanical and molecular regulation of bone remodeling. *Annu. Rev. Biomed. Eng.* 8, 455–498.
5. Zérath, E., Gryn timer, M., Holy, X., Viso, M., Patterson-Buckendahl, P., and Marie, P.J. (2002). Spaceflight affects bone formation in rhesus monkeys: a histological and cell culture study. *J. Appl. Physiol.* 93, 1047–1056.
6. Pereira Silva, J.A., Costa Dias, F., Fonseca, J.E., Canhao, H., Resende, C., and Viana Queiroz, M. (2004). Low bone mineral density in professional scuba divers. *Clin. Rheumatol.* 23, 19–20.
7. Van de Lest, C.H., Brama, P.A., and Van Weeren, P.R. (2003). The influence of exercise on bone morphogenic enzyme activity of immature equine subchondral bone. *Biorheology* 40, 377–382.
8. Koike, T. (2005). Evaluation of exercise as a preventive therapy for osteoporosis. *Clin. Calcium* 15, 673–677.
9. Hingorjo, M.R., Syed, S., and Qureshi, M.A. (2008). Role of exercise in osteoporosis prevention – current concepts. *J. Pak. Med. Assoc.* 58, 78–81.
10. Huang, T.H., Lin, S.C., Chang, F.L., Hsieh, S.S., Liu, S.H., and Yang, R.S. (2003). Effects of different exercise modes on mineralization, structure, and biomechanical properties of growing bone. *J. Appl. Physiol.* 95, 300–307.
11. Kim, C.S., and Park, D.H. (2005). Effects of chronic NH<sub>4</sub>Cl dosage and swimming exercise on bone metabolic turnover in rats. *J. Physiol. Anthropol. Appl. Human Sci.* 24, 595–600.
12. Kim, C.S., Nakajima, D., Yang, C.Y., et al. (2000). Prolonged swimming exercise training induce hypophosphatemic osteopenia in stroke-prone spontaneously hypertensive rats (SHRSP). *J. Physiol. Anthropol. Appl. Human Sci.* 19, 271–277.
13. Suominen, H. (2006). Muscle training for bone strength. *Aging Clin. Exp. Res.* 18, 85–93.
14. Swissa-Sivan, A., Statter, M., Brooks, G.A., et al. (1992). Effect of swimming on prednisolone-induced osteoporosis in elderly rats. *J. Bone Miner. Res.* 7, 161–169.
15. Devereux, K., Robertson, D., and Briffa, N.K. (2005). Effects of a water-based program on women 65 years and over: a randomised controlled trial. *Aust. J. Physiother.* 51, 102–108.
16. Carter, N.D., Khan, K.M., McKay, H.A., et al. (2002). Community-based exercise program reduces risk factors for falls in 65- to 75-year-old women with osteoporosis: randomized controlled trial. *Can. Med. Assoc. J.* 167, 1005–1006.
17. Matsumoto, T., Nakagawa, S., Nishida, S., and Hirota, R. (1997). Bone density and bone metabolic markers in active collegiate athletes: findings in long-distance runners, judoists, and swimmers. *Int. J. Sports Med.* 18, 408–412.
18. Bourrin, S., Ghaemmaghami, F., Vico, L., Chappard, D., Gharib, C., and Alexandre, C. (1992). Effect of a five-week swimming program on rat bone: a histomorphometric study. *Calcif. Tissue Int.* 51, 137–142.
19. Taba, M., Novaes, A.B., Souza, S.L.S., Grisi, M.F.M., Palioto, D.B., and Pardini, L.C. (2003). Radiographic evaluation of dental implants with different surface treatments: an experimental study in dogs. *Implant Dent.* 12, 252–258.
20. Placide, J., and Martens, M.G. (2003). Comparing screening methods for osteoporosis. *Curr. Womens Health Rep.* 3, 207–210.
21. Currey, J.D., Foreman, J., Laketic, I., Mitchell, J., Pegg, D.E., and Reilly, G.C. (1997). Effects of ionizing radiation on the mechanical properties of human bone. *J. Orthop. Res.* 15, 111–117.
22. Hanlon, E.B., Manoharan, R., Koo, T.W., et al. (2000). Prospects for in vivo Raman spectroscopy. *Phys. Med. Biol.* 45, R1–R59.
23. Moreira, L.M., Silveira Jr., L., Santos, F.V. et al. (2008). Raman spectroscopy: a powerful technique for biochemical analysis and diagnosis. *Spectrosc. Int. J.* 22, 1–19.
24. Park, C.S., Kim, K.K., Choi, J.M., and Park, K.S. (2007). Classification of glucose concentration in diluted urine using the low-resolution Raman spectroscopy and kernel optimization methods. *Physiol. Meas.* 28, 583–593.
25. Santos, R.S., Sidaoui, H.A., Silveira, L., Pasqualucci, C.A.G., and Pacheco, M.T.T. (2009). Classification system of Raman spectra using cluster analysis to diagnose coronary artery lesions. *Instrum. Sci. Technol.* 37, 327–344.
26. Nogueira, G.V., Martin, A.A., Zângaro, R.A., Pacheco, M.T.T., Chavantes, M.C., and Pasqualucci, C.A. (2005). Raman spectroscopy study of atherosclerosis in human carotid artery. *J. Biomed. Opt.* 10, 031117/1–031117/7.
27. Saade, J., Pacheco, M.T.T., Rodrigues, M.R., and Silveira, L. (2008). Identification of hepatitis C in human blood serum by near-infrared Raman spectroscopy. *Spectrosc. Int. J.* 22, 387–395.
28. Pilotto, S., Pacheco, M.T., Silveira Jr, L., Villaverde, A.B., and Zângaro, R.A. (2001). Analysis of near-infrared Raman spectroscopy as a new technique for a transcutaneous non-invasive diagnosis of blood components. *Lasers Med. Sci.* 16, 2–9.
29. Yuan, H., Yang, Z., Li, Y., Zhang, X., Bruijn, J.D., and Groot, K. (1998). Osteoinduction by calcium phosphate biomaterials. *J. Mater. Sci. Mater. Med.* 9, 723–726.
30. Carden, A., and Morris, M.D. (2000). Application of vibrational spectroscopy to the study of mineralized tissues (review). *J. Biomed. Opt.* 5, 259–268.
31. Lopes, C.B., Pinheiro, A.L., Sathaiah, S., Duarte, J., and Martins, C.M. (2005). Infrared laser light reduces loading time of dental implants: a Raman spectroscopic study. *Photomed. Laser Surg.* 23, 27–31.
32. Lopes, C.B., Pacheco, M.T., Silveira Jr, L., Duarte, J., Cangussú, M.C., and Pinheiro, A.L. (2007). The effect of the association of NIR laser therapy BMPs, and guided bone regeneration on tibial fractures treated with wire osteosynthesis: Raman spectroscopy study. *J. Photochem. Photobiol. B* 89, 125–130.
33. Timlin, J.A., Carden, A., and Morris, M.D. (1999). Chemical microstructure of cortical bone probe by Raman transects. *Appl. Spectrosc.* 53, 1429–1435.
34. Draper, E.R., Morris, M.D., Camacho, N.P., et al. (2005). Novel assessment of bone using time-resolved transcutaneous Raman spectroscopy. *J. Bone Miner. Res.* 20, 1968–1972.
35. Yerramshetty, J.S., and Akkus, O. (2008). The associations between mineral crystallinity and the mechanical properties of human cortical bone. *Bone* 42, 476–482.
36. Ramasamy, J.G., and Akkus, O. (2007). Local variations in the micromechanical properties of mouse femur: the involvement of collagen fiber orientation and mineralization. *J. Biomech.* 40, 910–918.
37. Schulmerich, M.V., Cole, J.H., Kreider, J.M., et al. (2009). Transcutaneous Raman spectroscopy of murine bone in vivo. *Appl. Spectrosc.* 63, 286–295.
38. McCreadie, B.R., Morris, M.D., Chen, T.C., et al. (2006). Bone tissue compositional differences in women with and without osteoporotic fracture. *Bone* 39, 1190–1195.
39. Gadeleta, S.J., Boskey, A.L., Paschalis, E., Carlson, C., Menschik, F., and Baldini, T. (2000). A physical, chemical, and



- mechanical study of lumbar vertebrae from normal, ovariectomized and nandrolone decanoate-treated cynomolgus monkeys (*Macaca fascicularis*). *Bone* 27, 541–550.
40. Voltarelli, F.A., Gobatto, C.A., and Mello, M.A.R. (2002). Determination of anaerobic threshold in rats using the lactate minimum test. *Braz. J. Med. Biol. Res.* 35, 1389–1394.
  41. Osorio, R.A., Silveira, V.L., Maldjian, S., Morales, A., Christofani, J.S., and Russo, A.K. (2003). Swimming of pregnant rats at different water temperatures. *Comp. Biochem. Physiol., Part A Mol. Integr. Physiol.* 135, 605–611.
  42. Osorio, R.A., Christofani, J.S., D'Almeida, V., Russo, A.K., and Picarro, I.C. (2003). Reactive oxygen species in pregnant rats: effects of exercise and thermal stress. *Comp. Biochem. Physiol., Part C Pharmacol. Toxicol.* 135, 89–95.
  43. Martins, M.V., da Silva, M.A., Medici Filho, E., de Moraes, L.C., Castilho, J.C., and da Rocha, R.F. (2005). Evaluation of digital optical density of bone repair in rats medicated with ketoprofen. *Braz. Dent. J.* 16, 207–212.
  44. Sakakura, C.E., Giro, G., Gonçalves, D., Pereira, R.M., Orri-co, S.R., and Marcantonio Jr., E. (2006). Radiographic assessment of bone density around integrated titanium implants after ovariectomy in rats. *Clin. Oral Implants Res.* 17, 134–138.
  45. Chatfield, C., and Collins, A.J. (1980). *Introduction to Multivariate Statistics*. London: Chapman & Hall.
  46. Paula Jr., A.R., Silveira, L., Pacheco, M.T. (2009). ProRaman: a program to classify Raman spectra. *Analyst* 134, 1203–1207.
  47. Hart, K.J., Shaw, J.M., Vajda, E., Hegsted, M., and Miller, S.C. (2001). Swim-trained rats have greater bone mass, density, strength, and dynamics. *J. Appl. Physiol.* 91, 1663–1668.
  48. Iwamoto, J., Takeda, T., and Ichimura, S. (1998). Effects of exercise on bone mineral density in mature osteopenic rats. *J. Bone Miner. Res.* 13, 1308–1317.
  49. Boivin, G., and Meunier, P.J. (2003). The mineralization of bone tissue: a forgotten dimension in osteoporosis research. *Osteoporos. Int.* 14, S19–24.
  50. Boskey, A.L., DiCarlo, E., Paschalis, E., West, P., and Mendelsohn, R. (2005). Comparison of mineral quality and quantity in iliac crest biopsies from high- and low-turnover osteoporosis: an FT-IR microspectroscopic investigation. *Osteoporos. Int.* 16, 2031–2038.

Address correspondence to:

Landulfo Silveira Jr.

Biomedical Engineering Center

Universidade Camilo Castelo Branco – UNICASTELO

Núcleo do Parque Tecnológico de São José dos Campos

Rod. Pres. Dutra, km 138

ZIP 12247-004, São José dos Campos, SP

Brazil

E-mail: landulfo.silveira@gmail.com;

landulfo.silveira@unicastelo.br